23rd ABCM International Congress of Mechanical Engineering
December 6-11, 2015, Rio de Janeiro, RJ, Brazil

METEOROLOGICAL MAST MOUNTED ON AN OFFSHORE OIL PLATFORM FOR WIND MEASUREMENT: A CFD ANALYSIS

Ezequiel Costa Malateaux da Silva
Rodrigo Dias
Petrobras Research Center (CENPES) - Gas, Power and Gas to Chemicals R&D Department, Av. Horácio Macedo, 950, Rio de Janeiro-RJ, Brazil
ezequiel.malateaux@petrobras.com.br, rodias@petrobras.com.br

Leonardo de Lima Oliveira
Luciano André Cruz Bezerra
CTGAS-ER - Centro de Tecnologias do Gás & Energias Renováveis, Av. Capitão-Mor Gouveia, 2770, Natal-RN, Brazil
leonardooliveira@ctgas.com.br, luciano@ctgas.com.br

Abstract. *In the last years, Brazil experienced an increase on power generation based on wind turbines. The gradual occupation of Brazilian high wind potential areas shows that, in the future, offshore wind turbines will probably be used in Brazil. Meteorological masts can be mounted on offshore platforms to acquire environmental data to evaluate the wind potential of specific sites, a strategy adopted by Petrobras, which installed the first offshore meteorological mast in Brazil. However, it is important to guarantee that the platform does not disturb the wind flow, which would result in false measured values for the wind speed. In the present work, a CFD simulation was performed to verify the impact of the platform on the wind flow. The results of the simulations were used to compare the values of the wind speed at the position of the meteorological mast with those of the non-disturbed flow, showing that the influence of the platform on the flow is very small for heights greater than 50 m.*

Keywords: *offshore wind energy, meteorological mast, computational fluid dynamics, offshore wind measurement*

1. INTRODUCTION

Wind is a very important renewable energy source in Brazil, a country where wind turbines are already responsible for an electric generation of about 6.4 GW (a number which has been increasing in last years). The total wind power estimated for Brazil is of 143.5 GW considering a high of 50 m (Amarante *et al*., 2001).

Areas with high wind potential are often preferred for constructing new wind energy parks. However, as these areas become rarer, entrepreneurs of this field start considering alternative areas, such as onshore fields with less attractive wind resources or even offshore fields. Thus, if the Brazilian offshore coast presents promising wind resources, it can be inferred that, in the next decades, offshore wind turbines will be a reality in Brazil. It is important to notice that the estimated offshore wind potential for Brazil is of 1780 GW and about 57 GW are located within 10 km from the coast. This shows a very important potential for the installation of offshore wind turbines in Brazil (Ortiz and Kampel, 2011).

Although offshore wind energy is very promising, the measurement of offshore environmental variables is required to evaluate whether or not a determined area is economic viable for the construction of an offshore wind park. The most used technique for evaluating onshore wind areas consists on mounting a mast in which are installed anemometers, wind vanes and other sensors (such as barometers, thermos hygrometers and pluviometers) to measure environmental data. Remote sensors, as LiDAR (Light Detection and Ranging), can also be used to acquire environmental data but the use of meteorological masts is still the most reliable method of wind potential measurement. Therefore, a previous offshore wind measurement using a meteorological mast would probably be required for the installation of an offshore wind park in Brazil, since a similar measurement is necessary for onshore wind parks.

In this way, Petrobras installed in 2013 the first offshore meteorological mast of Brazil. This mast was mounted on a deactivated rigid offshore oil platform located less than 50 km from the Rio Grande do Norte State coast. With more than 80 m high, this mast has five anemometers, three wind vanes, three barometers, three thermos hygrometers, one three dimensional ultrasonic anemometer and one pluviometer. The meteorological mast reaches 93 m regarding the ocean (considering the average ocean level). Figure 1 shows the meteorological mast mounted on the platform.

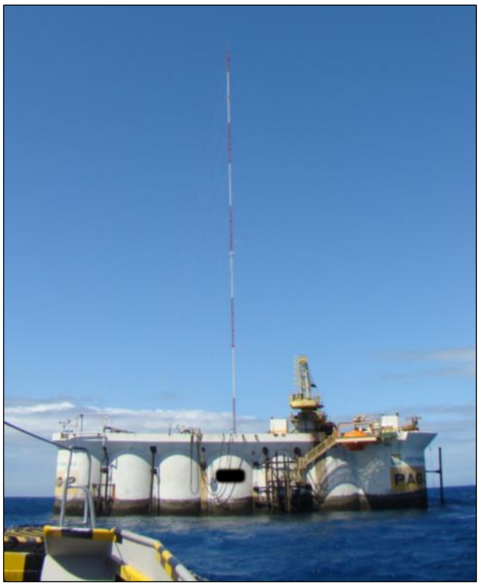

Figure 1. Meteorological mast mounted on the platform

The measured data must be as accurate as possible to predict the environmental behavior in the area. However, offshore wind turbines are not usually mounted on platforms such as the one where the meteorological mast was mounted. Thus, it is important to verify if the wind profile measured by the mast corresponds to the one of a non-disturbed flow, since the presence of the platform could change the flow field in some regions, leading to false wind velocity estimation by the mast.

In this work a CFD analysis was performed through the software OpenFOAM to evaluate the impact of the platform on the wind flow considering different wind directions and velocity profiles.

The velocity profile was analyzed at the position of the meteorological mast and then compared to the non-disturbed flow. The results show that the deviation above 50 m from the ocean level is lower than 4 %, showing that the offshore wind measurement by using a meteorological mast mounted on a platform provides results for the wind profile in the analyzed cases with a limited deviation.

Nomenclature

C_μ , C_{s1} , C_{s2}	K-epsilon constants
u	Velocity at x direction, [m/s]
u_*	Friction velocity at x direction, [m/s]
V_{xy}	Velocity at the xy plane, [m/s]
x, y, z	Cartesian coordinates, [m]
z_0	Aerodynamic roughness, [m]

Greek symbols

κ	Von Karman constant
σ_k	Turbulent Prandtl Number
σ_s	K-epsilon constant

2. METHODOLOGY

First, the procedure to determine the domain geometry and mesh will be described. Then, the boundary conditions and the turbulence model will be discussed. Next, the solver and convergence criteria will be described. The simulated cases will then be presented.

2.1 Definition of the domain and mesh generation

It was considered a prismatic domain (elongated at the wind direction) to analyze the wind flow around the platform. The domain dimensions were set as 800 m, 400 m and 350 m in x, y and z directions respectively. The horizontal dimensions of the platform are 53 m and 46 m, while its height above the ocean level is of 11 m approximately. The meteorological mast position, which is located at the center of the platform, was set at the center of the domain ($x = 400m$, $y = 200m$) to ensure that the boundaries would not interfere on the results at the position of the meteorological mast. Despite the fact that this strategy demands more computational time, it also saves time concerning the comparison of the results depending on the domain dimensions.

Once defined the domain dimensions, different meshes were created in order to evaluate the number of skew faces of each mesh. A skew face is a common error related to cell angles and it should be minimized. It was noted that the number of skew faces decreases with the z dimension of the domain. Table 1 presents the evaluated meshes and the number of skew faces of each one.

Table 1. Evaluated meshes

ID	Volumes in x direction	Volumes in y direction	Volumes in z direction	Number of skew faces
1	100	100	100	45
2	120	120	100	15
3	120	120	120	19
4	135	135	110	0

Given that the computational time for meshes more refined than mesh 4 was rapidly increasing, this mesh was chosen to perform the simulations. After that, the platform geometry was inserted at the domain by using the OpenFOAM's mesh generator *snappyHexMesh*. The resulting mesh is refined near the platform and near the ocean level. The approximate number of cells is 2250000. Figure 2 presents the interface between the mesh and the platform and ocean surfaces.

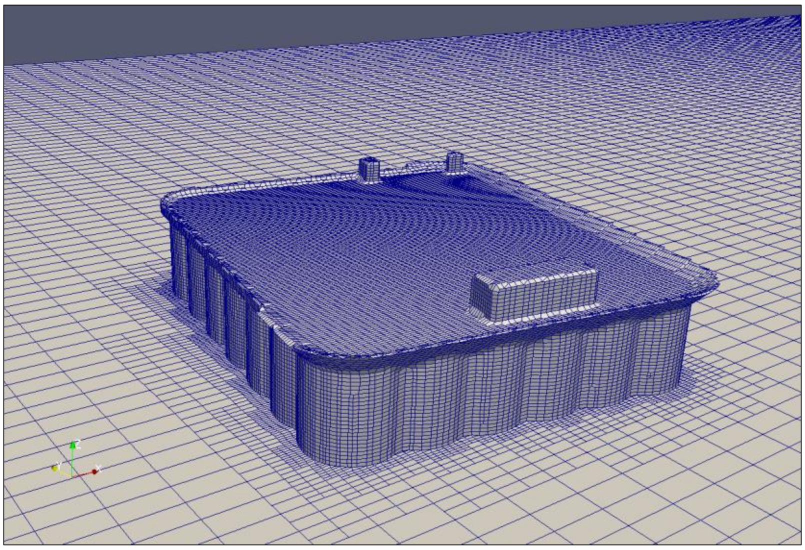

Figure 2. Interface between the mesh and the platform and ocean surfaces

2.2 Boundary conditions and turbulence model

The chosen domain has the following boundary conditions: the wind velocity inlet ($+x$), the pressure outlet ($-x$), three symmetry boundaries far from the platform ($-y$, $+y$ and $+z$), the ocean surface ($z = 0$) and the surfaces of the platform.

The most used turbulence model for wind simulations is the K-epsilon model. Thus, this model was chosen to represent the wind turbulence in this work. The model constants were set based on recommended values for simulations of atmospheric flows (Martinez, 2011): $\kappa = 0.41$, $C_\mu = 0.033$, $\sigma_\kappa = 1.00$, $C_{s1} = 1.21$ and $C_{s2} = 1.92$. The other constant, σ_s, was calculated from κ, C_{s1}, C_{s2} and C_μ.

The wind inlet was positioned at the highest x value. For the inlet, a log wind profile was considered, which is given by Eq. (1), which is commonly used to analyze wind flows (Blocken, 2007):

$$u = \frac{u_*}{\kappa} ln\left(\frac{z + z_0}{z_0}\right) \tag{1}$$

in which, u_* is the friction velocity at reference height, κ is the Von-Karman constant, z_0 is the aerodynamic roughness and u is the wind velocity at the height z. The wind velocity shown in this equation was also used to initialize the velocity value of all domain cells. The presented inlet velocity profile is set in the OpenFOAM software by specifying the inlet velocity as *atmBoundaryLayerInletVelocity*. For the pressure at the inlet boundary condition, *zeroGradient* was set to establish that the normal gradient pressure is zero. For the turbulent kinetic energy, the *uniformFixedValue* condition was set to determine that this parameter would be calculated at this position. For the turbulent kinetic energy dissipation, the *atmBoundaryLayerInletEpsilon* was set so epsilon would be calculated for this position regarding the position of each cell. The turbulent viscosity was set as *calculated* at this position.

As the platform was deactivated, the majority of the equipments were removed before the installation of the meteorological mast, but three structures with a considerable size remained on the platform. Therefore, those structures were added to the geometry, as can be seen in Fig. 2. There are also other small objects on the platform, but they were not included on the geometry due to limitations regarding the computing time. Thus, the impact of these objects was represented by considering a determined roughness for each surface of the platform. For the side wall of the platform, a roughness of 0.01 was chosen. On the top of the platform, a higher roughness of 0.02 was considered. For the ocean surface, a roughness of 0.0002 was considered. These values were chosen by comparison with roughness values summarized by Wieringa (1992a), a procedure used by many researchers (Wieringa, 1992b; Ramli *et al*., 2009; Ghahremani, 2013). For both platform and ocean surfaces, the same parameters were set in OpenFOAM for determining the variables. To ensure the no-slip condition, zero *uniformFixedValue* was set for the velocity. For the pressure, *zeroGradient* was set. For the turbulent kinetic energy and its dissipation, *KqRWallFunction* and *epsilonWallFunction* were respectively set. For the turbulent viscosity, the condition of *nutKAtmRoughWallFunction* was chosen in order to establish the calculation of the turbulent viscosity by using a wall function depending on the surface roughness.

The pressure outlet was positioned at the lowest x value. The *inletOutlet* condition was set for the velocity to treat this condition as an "opening", which could permit both outwards and inwards flow. The atmospheric pressure was determined by using *uniformFixedValue*. For the turbulent kinetic energy and its dissipation the *inletOutlet* was set. The turbulent viscosity was set as *calculated*.

The other domain surfaces were treated as *symmetry* boundary conditions since it is assumed that, due to the domain dimensions, there is no flow entering or exiting the domain through these boundaries. Thus, this type of boundary condition ensures that the flow is parallel to the boundaries in which it was used.

2.3 Simulation

The OpenFOAM solver used to simulate the studied cases was the *simpleFOAM*, a steady-state solver for incompressible, turbulent flow.

As the objective of this work is to provide an outlook about the influence of the offshore platform on the wind flow profile, buoyancy effects due to temperature differences (which impact the atmospheric stability) were not considered in this work.

An RMS criteria of 10^{-4} for momentum and mass conservation equations was adopted to determine the convergence of the solution.

2.4 Studied cases

The main objective of this work is to verify if the measured wind velocity by the anemometers installed at the mast corresponds to the wind velocity at the same height in a non-disturbed flow region. As the anemometers are calibrated for the range between $4\,m/s$ and $16\,m/s$, these values were chosen as reference to perform the simulations.

Based on Eq. (1), the friction velocity u_* was adjusted in order to make the wind velocity u equal to $4\,m/s$, $10\,m/s$ and $16\,m/s$ at 100 m high. Figure 4 presents the inlet velocities simulated until the height of 100 m.

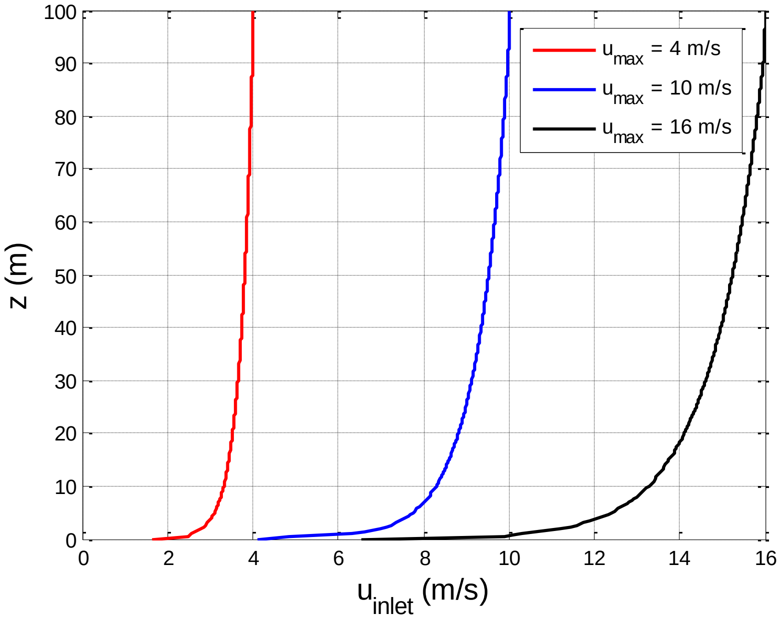

Figure 3. Inlet velocity profile for each case

For each velocity profile, three wind directions were simulated. For each direction, the geometry of the platform was turned around the mast axis while the external boundaries of the domain remained at their initial position. Figures 5a, 5b and 5c present a top view of the platform for each simulated direction. It should be remembered that the wind flows towards the $-x$ direction in all cases.

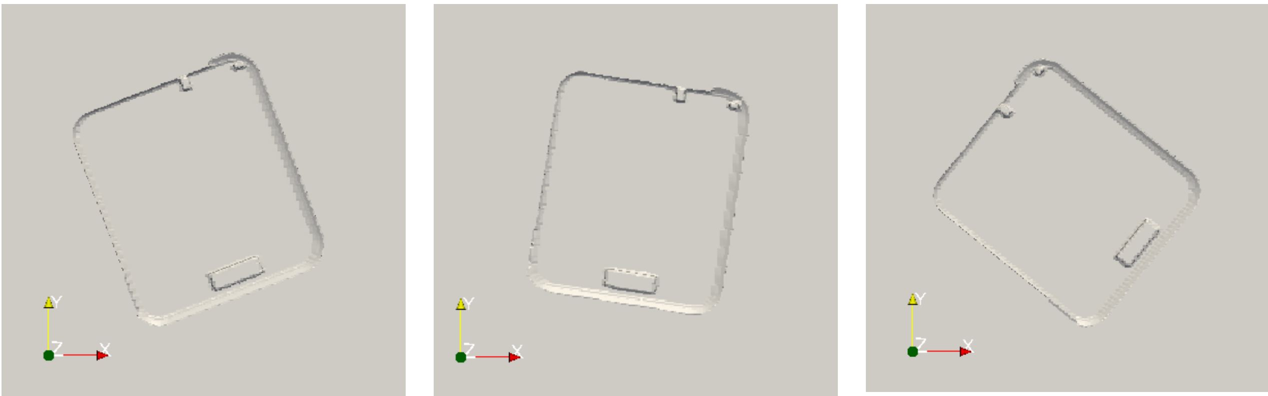

(a) (b) ©

Figure 4. Platform position for wind directions A, B and C respectively

3. RESULTS

It was used a convergence criteria of 10^{-4} for the root mean squared residuals of all solved equations (continuity, momentum, K and epsilon), criteria which was satisfied after about 1500 iterations for all cases.

Figure 6 shows the ratio between the horizontal velocity at the position of the meteorological mast and the velocity at the inlet for the same height z for all simulated cases.

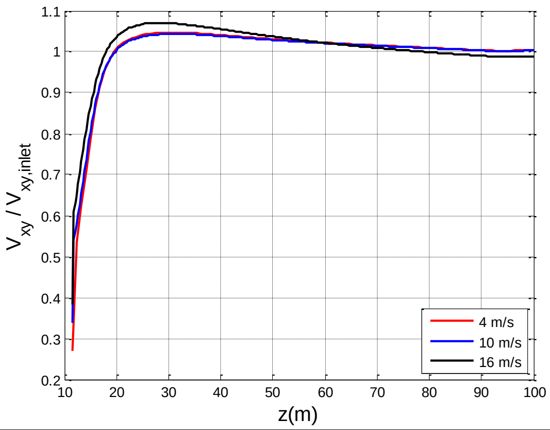

Height (m)	$V_{xy}/V_{xy,inlet}$ $u_{max} = 4m/s$	$u_{max} = 10m/s$	$u_{max} = 16m/s$
15	0,79	0,81	0,87
25	1,04	1,04	1,07
35	1,04	1,04	1,06
45	1,04	1,03	1,05
55	1,03	1,02	1,03
65	1,02	1,02	1,02
75	1,01	1,01	1,00
85	1,01	1,01	0,99
95	1,00	1,00	0,99

(a)

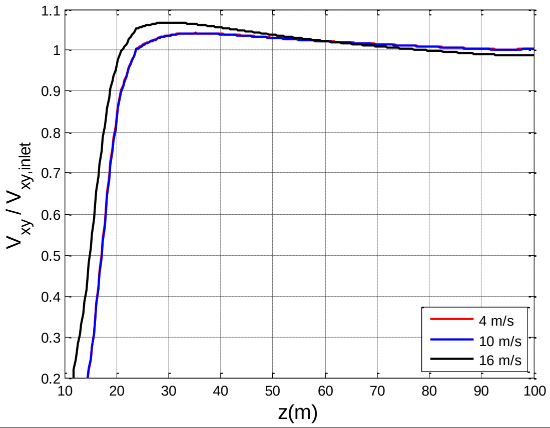

Height (m)	$V_{xy}/V_{xy,inlet}$ $u_{max} = 4m/s$	$u_{max} = 10m/s$	$u_{max} = 16m/s$
15	0,24	0,25	0,52
25	1,01	1,01	1,06
35	1,04	1,04	1,06
45	1,04	1,03	1,05
55	1,03	1,03	1,03
65	1,02	1,02	1,02
75	1,01	1,01	1,00
85	1,01	1,01	1,00
95	1,00	1,00	0,99

(b)

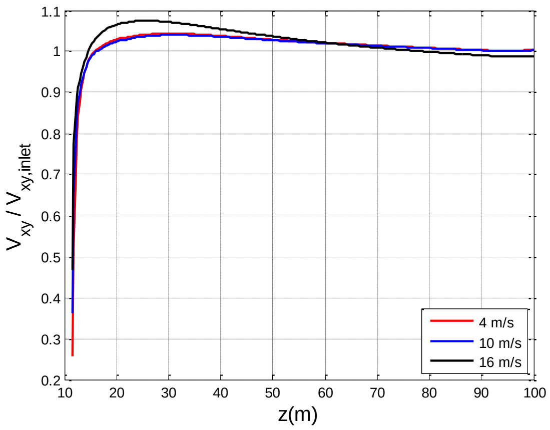

Height (m)	$V_{xy}/V_{xy,inlet}$ $u_{max} = 4m/s$	$u_{max} = 10m/s$	$u_{max} = 16m/s$
15	0,99	0,99	1,01
25	1,04	1,04	1,08
35	1,04	1,04	1,06
45	1,03	1,03	1,05
55	1,02	1,02	1,03
65	1,02	1,02	1,02
75	1,01	1,01	1,00
85	1,01	1,01	0,99
95	1,00	1,00	0,99

(c)

Figure 5. Ratio between the horizontal velocity at the meteorological mast and the inlet velocity for the same height for wind directions A, B and C respectively (the height z is measured from the ocean level)

As it can be seen on Fig. 6 for all wind profiles and directions, the velocity at the meteorological mast is much lower than the velocity of the non-disturbed flow for small heights. This is expected because some recirculation occurs in this region. As the height increases, the wind velocity at the meteorological mast first becomes higher than the velocity of the non-disturbed flow and then the velocity ratio tends to the unity value, meaning that the measured data at the meteorological mast is less affected by the presence of the platform for elevated heights. Furthermore, it can be seen that, for all wind directions, the inlet wind velocity profile with $u_{max} = 16m/s$ provided the highest distortions regarding the non-disturbed flow.

It can also be seen on Fig. 6 that the wind direction B is the one that presents the highest distortion on the wind flow for small heights. This happened because in this case the recirculation above the platform is more important due to the perpendicularity between the wind main direction and one of the platform sides. Due to the same fact, the simulation results for direction A presents a greater distortion than the simulation results for direction C for small heights. This can be seen on Fig. 7, which presents the velocity field for all wind directions for the inlet wind profile in which $u_{max} = 16 m/s$:

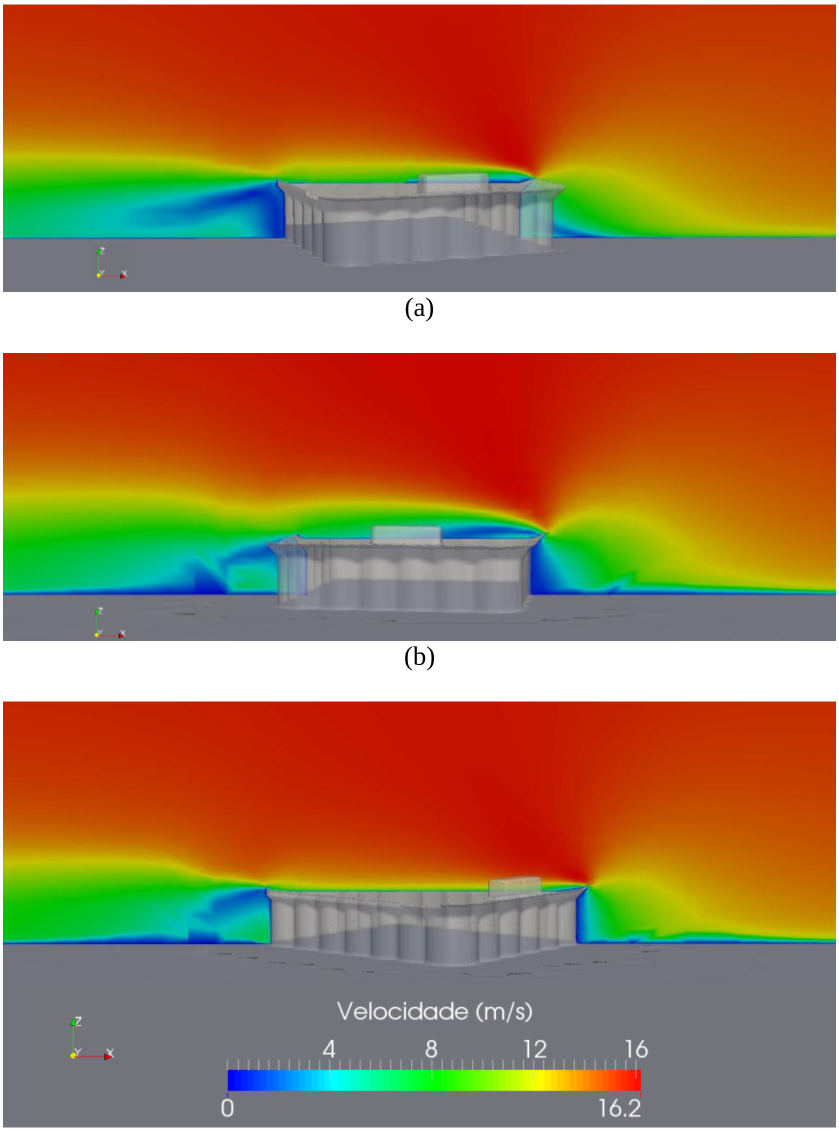

(a)

(b)

(c)

Figure 6. Velocity field for the inlet wind profile in which $u_{max} = 16 m/s$: wind directions A, B and C respectively

For all cases, it can be noticed that the deviation between the wind velocity at the mast position and the inlet wind velocity for heights above 22 m is lower than ± 10 % and for heights above 50 m is lower than 4 %.

4. CONCLUSION

A CFD study was performed considering different wind profiles and wind directions to verify the influence of the platform on the wind velocity measured by the anemometers disposed at the meteorological mast.

It was verified that the wind flow near the platform presents much lower velocities than the non-disturbed flow for all wind profiles and directions simulated. The ratio between wind velocities increases with the height and, for heights greater than 22 m, the velocity at the mast position corresponds to the velocity of the non-disturbed flow with an error of ± 10 % for all wind directions and inlet wind profiles. Also for all directions and inlet profiles, the difference between the mast and the non-disturbed velocities becomes lower than 4 % after the height of 50 m. These deviations could be used to correct the energy production estimation from measured wind data.

Another important fact is that the wind direction also impacts the measured velocity at the meteorological mast: wind direction B leads to a higher distortion on the wind flow for small heights than the other directions due to the perpendicularity between the wind main direction and one of the sides of the platform.

From the results, it can be inferred that, for different wind profiles, the measured wind velocity by anemometers positioned at heights above 50 m (from the ocean level) presents values next to the ones of the non-disturbed flow (deviation lower than 4 %) for the simulated wind directions.

For future works, it is suggested the evaluation of the impact of different meshes on the results in order to provide an even better confidence of the results.

5. ACKNOWLEDGEMENTS

The authors would like to thank Petrobras which funded this research through the project P&D "Aperfeiçoamento de Modelo para Avaliação de Potencial Eólico Offshore", developed under the Programme for Research and Technological Development of the Power Sector regulated by ANEEL (National Electric Energy Agency).

6. REFERENCES

Amarante, O.A.C., Brower, M., Zack, J. and Sá A.L., 2001. *Atlas do Potencial Eólico Brasileiro*. Ministério de Minas e Energia, Brasília, Brazil.

Blocken, B., Stathopoulos T., Carmeliet, J., 2007. "CFD Simulation of the Atmospheric Boundary Layer: Wall Function Problems". *Atmospheric Environment*. 41, p. 238-252.

Ghahremani, R., 2013. *CFD simulation of Wind Condition and Thermal Gradient around an Offshore Helideck*. Master's thesis, University of Stavanger, Stavanger, Norway.

Martinez, B., 2011. *Wind Resource in Complex Terrain with OpenFOAM*. Master's thesis, Technical University of Denmark, Lyngby, Denmark.

Ortiz, G.P. and Kampel, M., 2011. "Potencial de Energia Eólica Offshore da Margem do Brasil". In *V Simpósio Brasileiro de Oceanografia*. Santos, Brazil.

Ramli, N.I., Ali, M.I., Saad, M.S.H., Majid,T.A., 2009. "Estimation of the Roughness Length (z_o) in Malaysia Using Satellite Image". In *VII Asia-Pacific Conference on Wind Engineering*. Taipei, Taiwan.

Wieringa, J., 1992. *Representative Roughness Parameters for Homogeneous Terrain*. Royal Netherlands Meteorological Institute, De Bilt, Netherlands.

Wieringa, J., 1992. "Updating the Davenport Roughness Classification". *Journal of Wind Engineering and Industrial Aerodynamics*. 41-44, p. 357-368.

7. RESPONSIBILITY NOTICE

The authors are the only responsible for the printed material included in this paper.